East European Journal of Physics. 1. 460-472 (2026)
DOI:10.26565/2312-4334-2026-1-53 ISSN 2312-4334

A STUDY ON THERMO-VISCOUS STEADY FLUID MOTION THROUGH A MOVING RECTANGULAR FLAT PLATE-A NUMERICAL APPROACH

N. Pothanna[1], P. Raja Shekar[1]*, Jyotsna Cherukuri[2], L. Srinivasa Rao[3], Adigoppula Raju[4], Devunuri Suresh[5]

[1]*Department of Mathematics, VNR Vignana Jyothi Institute of Engineering and Technology, Hyderabad, Telangana, India-500090*
[2]*Department of Chemistry, VNR Vignana Jyothi Institute of Engineering and Technology, Hyderabad, Telangana, India-500090*
[3]*Centre for Nanoscience and Technology, Department of Physics, VNR Vignana Jyothi Institute of Engineering and Technology, Bachupally, HYD., TG, India -500 090*
[4]*Department of Applied Sciences, Symbiosis Institute of Technology, Symbiosis International (Deemed University), Pune-412115, India*
[5]*Department of Automobile Engineering, VNR Vignana Jyothi Institute of Engineering and Technology, Hyderabad, Telangana, India-500090*
**Corresponding author E-mail: rajoct25@gmail.com*
Received November 19, 2025; revised December 25, 2025; accepted January 21, 2026

This study presents a novel numerical approach for analysis on thermo-viscous steady fluid motion through a moving rectangular flat plate. The numerical results have been found employing the Runge-Kutta method of order 6 shooting techniques developed in *Mathematica* software. Numerical differentiation (ND) solves for the flow-adaptable equations comprising temperature and velocity. The flow behavior and the impacts of material constraints on the flow region for governed equations have been analyzed and deliberated, taking the help from the generated graphs. The nonlinear coupled Partial differential equations (PDE's) in terms of temperature and velocity, subject to the corresponding boundary conditions, control the fluid motion. The numerical computations of Runge-Kutta(R-K) 6^{th} order results are presented in form of tables and also represented for numerous thermophysical coefficient values. The variations of these flow fields have been studied for wide spectrum of physical characteristics which influences the nature of thermo-viscous fluid. The impact of suction/injection parameter, dimensionless viscosity factor, constant pressure and temperature gradients, thermophysical factors and the Prandtl parameter effect on flow region have explored using graphical illustrations with the wide range of values. The Explicit numerical calculations also been calculated and results are associated through the current outcomes in the literature. To improve heat transfer rates in systems such as heat exchangers and aerospace components, engineers can optimize surface textures and flow conditions by taking coefficients effects on flow considerations into account.
Keywords: *Thermo-viscous fluid; ND Solve; R-K 6^{th} order Method; Permeability; Thermal Conductivity*
PACS: 02.30. Hq, 02.30.Jr, 02.60.Cb, 02.60.Lj

Nomenclature

$\alpha_1 = -p$	Pressure of Fluid	d_{ij}	Deformation rate tensor
$\alpha_3 = 2\mu$	Viscosity Coefficient	b_{ij}	Thermal gradient bi-vector
$\alpha_5 = 4\mu_c$	Cross model viscosity parameter	t_{ji}	Stress tensor
α_6	Thermo interaction stress coefficient	h	Thermo bi-gradient of vector
α_8	Thermal viscosity stress parameter	T	Temperature (non-dimensional)
$\beta_1 = k$	Fourier and thermal conductivity Coefficient	U	Dimensionless velocity
β_3	Thermal strain factor of conductivity	V	Dimensionless injection/ suction parameter
a_6	Thermal interaction stress factor (non-dimensional)	C_1	Pressure gradient that is constant
b_3	Thermal strain coefficient of conductivity(non-dimensional)	C_2	Temperature gradient that is constant
v_o	Injection/suction parameter		**Greek Symbols**
p_r	Prandtl number	ρ	Fluid Density
c	Specific heat	γ	External Source energy per unit mass
f_i	i^{th} component of external force per unit mass	η	Temperature of a Fluid
q_i	i^{th} component of heat flux bi-vector	$\alpha_i's$	Coefficient of viscosity
u_i	i^{th} velocity component	$\beta_i's$	Coefficient of thermal conductivity

1. INTRODUCTION

The features of non-Newtonian fluid have been a subject of substantial investigation for centuries. However, it is only during the last six to seven decenniums particularly since the second world war time, the significant research efforts have been undertaken to expand these evaluates into the non-linearity domain. The non-linear thermo-viscoelasticity

Cite as: N. Pothanna, P.R. Shekar, C. Jyotsna, L.S. Rao, A. Raju, D. Suresh, East Eur. J. Phys. 1, 460 (2026), https://doi.org/10.26565/2312-4334-2026-1-53

fundamentals were considered by Koh and Eringen [1]. Yamamoto et al. [2] investigated convective acceleration in flow through a porous wall. Conditions near a naturally porous wall's boundaries were considered by Beavers et al. [3]. In thermodynamics, the existence of caloric equations of state was examined by Coleman et al. [4]. A few incompressible viscometric flows of thermo viscous fluids were described by Kelly [5]. A thermo-viscous fluid of second-order flowing steadily across an endless plate was examined by Rao et al. [6]. Unsteady thermo viscous movement over a staggering horizontal plate in a permeable slab was investigated by Pothanna and Aparna [7]. In this work they demonstrated the analytical expressions and solutions for the governed flow equations. The effect of heat production during flow of nanofluids across a shrieking sheet was inspected by Jithender Reddy et al. [8]. Thermo-viscous liquid movement in a permeable wedge enclosed by the comparative mobility of two impermeable extending equal plates was examined by Pothanna et al. [9]: four-stage algorithmic methodology. Employing this methodology, the external forces applied and internal energy sources generated have been calculated in this work. Considering a viscous effect, chemical response, and Soret-Dufour constraints, Kumar et al. [10] examined the behavior of heat-mass transfer in a 2-D forchheimer permeable region on casson mhd fluid flow across a disposed non-linear surface. Pothanna [11] used an analytical and numerical method to study an unsteady fluid flow around an oscillating sphere. The casson mhd nanofluid and the impact of thermal radiation with the presence of chemical reaction on the flow over a non-linear elongating sheet was described by Shekar et al. [12]. Using artificial neural networks, Pothanna et al. [13] investigated instable thermo viscid liquid transport among two indefinitely stretched impervious straight plates. This work compares to other literature works related to the flow between parallel plates is analyzed deeply with the statistical analysis on the required flow fields with the data-driven neural networks approach. Nalimela et al. [14] used artificial neural network techniques to forecast and assess an instable liquid flow over a horizontal oscillating plate in an absorbent slab. The radially inflow and outflow of a viscous hydromagnetic fluid concerning two narrow flat disks were investigated by Naeem et al. [15]. The entropy creation in heated joule radiation viscous fluid flow over a permeable radially extending disk was investigated numerically by Tahir et al. [16]. The mhd electronic effect on Darrcy-Forchheimer fluid flow on a stretchy surface was investigated by Zeeshan et al. [17] using an integrated intelligent neuro-evolutionary computing technique. The incompressible viscous fluid flow determined by a pressure differential in a specific channel was examined by Hranislav et al. [18]. The heat-mass transfer case study for a viscous fluid flow in a double layer caused by ciliate channel was completed by Nahid et al. [19]. The influence of blowing or suction on the temperature distribution and flow velocity across a flat plate is observed by Ahmed et al. [20]. The effects of chemical reactions and diffusion on heat transmission in casson nano-fluid flowing across a plane plate with accretion were investigated by Jayaprakash et al. [21]. The compressible mhd flow on plane plate boundary layer flow with somewhat exclusive effects was investigated by Shunhao et al. [22]. The use of a multi-test technique to simultaneously determine the adiabatic temperature near the wall and heat transfer effect in a shock channel for transonic flow across a flat plate was described by Wei et al. [23]. The Buongiorno nano fluid model's numerical calculations for the viscoelastic boundary layer flow of a towards a non-linear extending sheet were completed by Sohail et al. [24]. The study of magnetic fields and temperature radiation on dusty tangent hyperbolic fluid flow on an elongating sheet with a high prandtl number were investigated by Ali et al. [25]. The effects of Newtonian heating and slip conditions on mhd flow of a casson fluid across a nonlinearly stretching sheet saturated in a porous media were examined by Imran et al. [26]. In mhd casson fluid flow via a wavering vertical plate absorbed in a porous region with ramping wall temperature, Hari et al. [27] described heat-mass transfer. The impact of a heat cause and chemical response on the dissipative mhd mixed convection flow of a casson nano fluid across a non-linear permeable stretch sheet was examined by Ibrahim et al. [28]. The maxwell fluid through an infinite plate was explored with a novel exact solution by Fetecau et al. [29]. Dholey [30] investigated the first Stokes issue, which is flow caused by an infinite flat plate that abruptly starts moving in a viscoelastic fluid.

The thermo-viscous incompressible flows typically satisfy the succeeding governing equations:

Continuity equation formula: $v_{i,i} = 0$

Momentum equation formula:

$$\rho\left[\frac{\partial \mathrm{v_i}}{\partial \mathrm{t}} + \mathrm{v_k v_{i,k}}\right] = \rho \mathrm{f_i} + \mathrm{t_{ji,j}}$$

and the energy calculation formula:

$$\rho c\dot{\theta} = t_{ij} d_{ij} - q_{i,i} + \rho\gamma$$

where $\mathrm{f_k}$ is external forces per mass unit (k^{th} Component), t_{ij} is the stress component tensor and d_{ij} is components rate deformation tensor.

A fluid that is viscous in a thermal state, known as a thermo-viscous fluid, is defined by a pair of equations that constitute: one for heat and another for stress. The kinematic tensor's polynomial functions are the heat flux bi-vector (h) and stress tensor (t), which also includes deformation rate of tensor d, thermo bi-gradient of vector b, density ρ and the temperature θ

$$b \equiv \|b_{ij}\| \equiv \|\varepsilon_{ijk}\, \theta_{,k}\|$$

$$h \equiv \|h_{ij}\| \equiv \|\varepsilon_{ijk}\, q_{,k}\|$$

where ε_{ijk} illustrating the sign for permutation.

Stated differently, for thermo-viscous liquids,

$$\overrightarrow{t} = \overrightarrow{t}(d, b, \rho, \theta), \text{ and } \overrightarrow{h} = \overrightarrow{h}(d, b, \rho, \theta)$$

The mechanical equivalences for the heat flux bivector and stress tensor provided by Koh and Eringen [1] are

$$t = \alpha_1 I + \alpha_3 d + \alpha_5 d^2 + \alpha_6 b^2 + \alpha_8 (db - bd) + \alpha_{12} (db^2 - b^2 d) + \alpha_{15} (bd^2 - d^2 b) + \alpha_{17}(d^2 b^2 - b^2 d^2) + \alpha_{20}(dbd^2 - d^2 bd) + \alpha_{22}(bdb^2 - b^2 db) + \alpha_{24}(bd^2 b^2 - b^2 d^2 b)$$

and

$$h = \beta_1 b + \beta_3(bd + db) + \beta_6(db^2 - b^2 d) + \beta_9(bd^2 + d^2 b) + \beta_{12}(d^2 b^2 - b^2 d^2) + \beta_{19}(db^2 d^2 - d^2 b^2 d)$$

the constitutive coefficient $\alpha_i'^s$ and $\beta_i'^s$. These polynomials in the d and b invariants along these lines:

$$tr\, d\,, tr\, d^2, tr\, d^3, tr\, b^2$$

$$tr\, db^2, tr\, d^2 b^2, tr\, bdb^2 d^2$$

with coefficients depending on ρ and θ only.

The combined degree is N+P where N and P represent the maximum of the degrees of d and b in the aforementioned fundamental formulas.

In this illustration, Max |N+P|=2. The constitutive fundamental formulas are therefore joined in d and b as

$$t = \alpha_1 I + \alpha_3 d + \alpha_5 d^2 + \alpha_6 b^2 + \alpha_8 (db - bd)$$

and

$$h = \beta_1 b + \beta_3(bd + db)$$

with the deformation rate tensor: $d_{ij} = (u_{i,j} + u_{j,i})/2$ and bivector gradient 'b': $b_{ij} = \in_{ijk} \theta_k$

where u_i is the i^{th} fluid's velocity component and θ is the fluids temperature.

The constants α_i and β_i are polynomial expressions in terms of d and b are coefficients that are entirely be contingent on θ and ρ. The constants such as α_1 and α_3 can be determined as pressure of fluid and viscosity constant coefficient correspondingly and α_5 is the cross-viscosity coefficient. The expressions for the constitutional coefficients $\alpha_i'^s$ and $\beta_i'^s$ in the second order concept can be attained as

$$\alpha_1 = \alpha_{1000} + \alpha_{1010} tr\, d + \alpha_{1020} tr\, d^2 + \alpha_{1002}\, tr\, b^2\,, \alpha_3 = \alpha_{3010} + \alpha_{3020} tr\, d,$$

$$\alpha_5 = \alpha_{5020}\,, \alpha_6 = \alpha_{6002}\,, \alpha_8 = \alpha_{8011}\,, \beta_1 = \beta_{1001} + \beta_{1011} tr\, d \text{ and } \beta_3 = \beta_{1011}$$

the second order coefficients α_{isrt} and β_{isrt} are functions in terms of ρ and η.

In this work, the properties of different material characteristics on the thermo-viscous steady flow fields of a fluid through a horizontal moving flat plate are attempted to be studied. The current study was greatly helpful to the scientist and researchers to resolve their engineering and research study problems. The last several years have seen a huge increase in interest in the investigation of the flow features of these formations due to the vast range of applications.

1.1 Novelty and Research gap

This study investigates a novel numerical approach for analysis on thermo-viscous steady fluid motion through a moving rectangular flat plate for application of non-Newtonian fluids in aerospace engineering. Analysis has been done on the effects of different thermo-viscous characteristics with the development of ND solve developed algorithms. These fluids were the subject of earlier attempts in the literature, but the non-linear nature of the studies they included was not taken into consideration. The non-linear fluid behavior with various impacts have been studied and analyzed with the development of this algorithm. This present work developed to study the non-linear nature of the fluid using Mathematica software ND solve. The literature has not yet addressed this present work.

2. MATHEMATICAL MODELING

Consider the thermo-viscous steady fluid flow through permeable stretched infinite plate bounded in a impermeable medium as shown in Fig. (1). A study is conducted on the movement of the plate in the flow direction, moving at a specific velocity u_0. In the system of coordinates O(XYZ), the plates can be denoted by $y = 0$ and $y = \infty$. The points on x-axis are in the plate movement direction, the y-axis is vertical to the plates, and the origin is on the fixed plate. Further, a constant temperature of θ_0 and θ_1 is maintained accordingly.

Consider the fluid velocity $[u(y), v_0, 0]$ also fluid temperature θ(y) define the steady constant motion through a moving flat plate. The continuity calculation is fulfilled with this velocity choice.
The fundamental equations that describe the flow as follows:
along the X-direction:

$$\rho v_0 \frac{\partial u}{\partial y} = -\frac{\partial p}{\partial x} + \mu \frac{\partial^2 u}{\partial y^2} - \alpha_6 \frac{\partial \theta}{\partial x}\frac{\partial^2 \theta}{\partial y^2} + \rho F_x \tag{1}$$

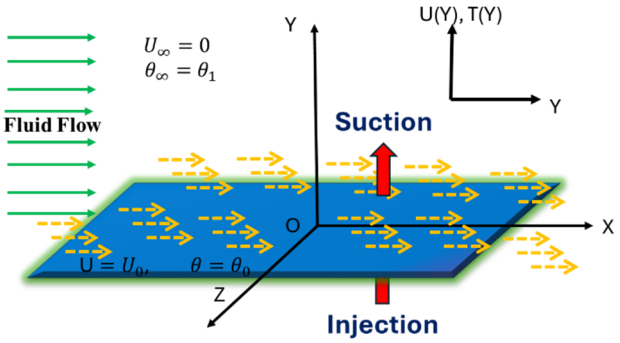

Figure 1. Flow Configuration

The fluid in the x-direction by the rate of change of fluid velocity with effect of plate suction/injection is represented by the term $\rho v_0 \frac{\partial u}{\partial y}$. The fluid is pushed in the x-direction by the rate of change of fluid pressure, with regard to the term $\frac{\partial p}{\partial x}$. Momentum diffusion caused by viscosity is represented by the viscous term $\mu \frac{\partial^2 u}{\partial y^2}$. Because of the internal resistance that shifts momentum from high to low regions, this attempts to smooth out velocity gradients. Boundary-layer growth, flow separation, vortex formation, and shock boundary layer interaction on wings are all governed by changes in temperature, which are represented by the second order nonlinear convective acceleration term ($\alpha_6 \frac{\partial \theta}{\partial x}\frac{\partial^2 \theta}{\partial y^2}$).

Along the Y-direction:

$$0 = \mu_c \frac{\partial}{\partial y}\left(\frac{\partial u}{\partial y}\right)^2 + \rho F_y \tag{2}$$

Along Z- direction:

$$0 = \alpha_8 \frac{\partial}{\partial y}\left(\frac{\partial \theta}{\partial y}\frac{\partial u}{\partial y}\right) + \rho F_z \tag{3}$$

and energy equation is

$$\rho c\left(u\frac{\partial \theta}{\partial x} + v_0 \frac{\partial \theta}{\partial y}\right) = \mu\left(\frac{\partial u}{\partial y}\right)^2 - \alpha_6 \frac{\partial \theta}{\partial x}\frac{\partial u}{\partial y}\frac{\partial \theta}{\partial y} + k\frac{\partial^2 \theta}{\partial y^2} + \beta_3 \frac{\partial \theta}{\partial x}\frac{\partial^2 u}{\partial y^2} + \rho\gamma \tag{4}$$

The convective expression $\rho c\left(u\frac{\partial \theta}{\partial x} + v_0 \frac{\partial \theta}{\partial y}\right)$ illustrates how heat is transported by a flowing fluid. The thermal conduction through the fluid is given by the conductive term $k\frac{\partial^2 \theta}{\partial y^2}$. The internal heat generation resulting from fluid friction is represented by the viscous dissipation term $\mu\left(\frac{\partial u}{\partial y}\right)^2$. The effects of thermal conductivity(β_3) and thermo-viscosity(α_6) on fluid flow are caused by the terms $\beta_3 \frac{\partial \theta}{\partial x}\frac{\partial^2 u}{\partial y^2}$ and $\alpha_6 \frac{\partial \theta}{\partial x}\frac{\partial u}{\partial y}\frac{\partial \theta}{\partial y}$ respectively.

In high-speed or high-shear regions, the second-order nonlinearities become significant because they couple velocity and temperature through viscous dissipation, thermal conductivity, and thermo viscosity factors. Accurate modeling of these nonlinear terms is crucial for predicting performance, guaranteeing structural integrity, and optimizing wing shapes in transonic and supersonic regimes because they dictate how aerodynamic heating, temperature gradients, and compressibility effects interact with the flow field for aircraft wings, influencing lift, drag, thermal loads, and material limits.

The boundary limitations assumed are:

$u = u_0$, $\theta = \theta_0$ at $y = 0$

and

$$u = 0, \theta = \theta_1 \text{ at } y = \infty \tag{5}$$

It is assumed that the plate velocity is constant. There are many real-world and useful uses for this in the field of aerospace engineering. This condition often applies at the wing surfaces to evaluate air flow over wings, which is crucial

for aircraft design in order to efficiently forecast flow behavior. Shear stress and viscosity-related energy losses in turbine and compressor jet engines are predicted by this condition. The boundary conditions for temperature are considered to be constants. These boundary conditions are essential for simulating conduction, convection, and radiation because they specify how temperature changes at the fluid-surface contact.

The dimensionless quantities were introduced as follows:

$$y = hY\ ,\ u = \frac{\mu}{\rho h}U\ ,\ u_0 = (\frac{\mu}{\rho h})\ U_0,\ T = \frac{\theta-\theta_0}{\theta_1-\theta_0}\ ,\ \frac{\partial\theta}{\partial x} = \frac{\theta_1-\theta_0}{h}C_2,\ \frac{\partial p}{\partial x} = \frac{\mu^2}{\rho h^3}C_1,\ p_r = \frac{\mu c}{k},\ b_3 = \frac{\beta_3}{\rho h^2 c}\ ,\ a_6 = \frac{\alpha_6\rho(\theta_1-\theta_0)^2}{\mu^2}$$

and $V = \frac{v_0\rho h}{\mu}$

where C_1 and C_2 are dimensionless pressure and temperature gradients respectively. V is the injection/ suction parameter.

When the pressure gradient, outside forces, and internal energy source are removed, the aforementioned non-dimensional quantities can be used to reduce equations (1) and (4) to

$$V\frac{dU}{dY} = -C_1 + \frac{d^2U}{dY^2} - a_6C_2\frac{d^2T}{dY^2} \tag{6}$$

$$UC_2 + V\frac{dT}{dY} = a_1\left[\left(\frac{dU}{dY}\right)^2 - A_6C_2\frac{dU}{dY}\frac{dT}{dY}\right] + b_3C_2\frac{d^2U}{dY^2} + \frac{1}{p_r}\frac{d^2T}{dY^2} \tag{7}$$

in addition to the boundary limitations:

$$U(0) = 1\ ,T(0) = 0 \tag{8}$$

and

$$U(\infty) = 0\ ,T(\infty) = 1 \tag{9}$$

3. NUMERICAL SCHEME

The second order linear ordinary differential equations (6 and 7) which have been obtained are coupled with velocity and temperature fields. The solutions of differential equations governed by the equations (6 and 7) by employing the b. c's (8 and 9) for velocity and temperature were measured using the MATHEMATICA ND solver tool package via. shooting technique with 6th order R-K methods and its solution flow chart is presented in Fig. 2. Following the introduction of dimensional-less quantities into the fluid equations, the infinite distance from the plate is represented by the units "h" for temperature and velocity (i.e., y→h) has been reduced to a finite value of 10. The solution's convergence was confirmed to meet the problem's boundary circumstances. Tables and illustrations have been used to display the impact of diverse material constants for the velocity and temperature of the fluid, including the suction/injection(V), coefficient of thermal interaction stress coefficient(a_6), thermal strain coefficient of conductivity (b_3), cross viscosity parameter (μ_c) , Prandtl parameter(p_r), non dimensional viscosity (a_1), specific heat (c), density (ρ), constant pressure gradient (C_1) and constant temperature gradient (C_2).

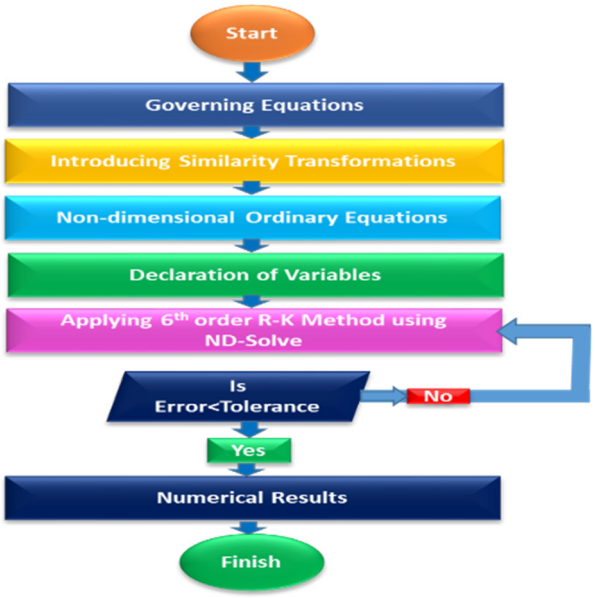

Figure 2. Flow Chart

3.1. Tables

The numerical outcomes related with the several substantial properties are shown in table.1 and table.2 and deliver the governing equations' explanations of fluid ascribed in temperature also velocity fields. The MATHEMATICA ND solver tool has yielded the numerical results of the equations that govern (6) and (7) with regard to the b.c.'s (8–9).

Table 1. Numerical computations for the velocity $U(Y)$ and temperature $T(Y)$ for V

Y	$U(Y)$ $a_6 = 0.01, b_3 = 0.10, C_1 = 0.2, C_2 = 0.2, a_1 = 0.1, p_r = 0.77$				$T(Y)$ $a_6 = 0.01, b_3 = 0.10, C_1 = 0.2, C_2 = 0.2\ a_1 = 0.1, p_r = 0.77$			
	V=0.10	V=0.25	V=0.50	V=0.75	V=0.10	V=0.25	V=0.50	V=0.75
0.00	1.00000	1.00000	1.00000	1.00000	0.00000	0.00000	0.00000	0.00000
1.00	0.16455	0.16537	0.1719	0.18216	1.05873	1.26153	2.25314	3.18553
2.00	-0.54864	-0.54699	-0.53375	-0.51286	2.01654	2.4126	4.35037	6.17665
3.00	-1.12689	-1.1245	-1.10532	-1.07494	2.7891	3.34351	6.05701	8.61842
4.00	-1.55611	-1.55319	-1.52961	-1.49213	3.31694	3.97622	7.20413	10.25492
5.00	-1.82073	-1.81753	-1.79165	-1.75046	3.56478	4.26379	7.68744	10.92698
6.00	-1.90345	-1.90028	-1.87462	-1.83373	3.52108	4.18983	7.46673	10.57118
7.00	-1.78512	-1.7823	-1.75955	-1.72326	3.19746	3.76812	6.56592	9.22002
8.00	-1.44451	-1.44238	-1.42515	-1.39767	2.62823	3.04228	5.07363	7.0035
9.00	-0.85814	-0.85697	-0.84755	-0.83253	1.86981	2.08546	3.14432	4.15189
10.0	0.00000	0.00000	0.00000	0.00000	1.00000	1.00000	1.00000	1.00000

Table 2. Numerical computations for the velocity $U(Y)$ and temperature $T(Y)$ for C_1

Y	$U(Y)$ $a_6 = 0.01, b_3 = 0.10, V = 0.25, C_2 = 0.2, a_1 = 0.1, p_r = 0.77$				$T(Y)$ $a_6 = 0.01, b_3 = 0.10, V = 0.25, C_2 = 0.2, a_1 = 0.1, p_r = 0.77$			
	C1=0.10	C1=0.30	C1=0.50	C1=0.70	C1=0.10	C1=0.30	C1=0.50	C1=0.70
0.00	1.00000	1.00000	1.00000	1.00000	0.00000	0.00000	0.00000	0.00000
1.00	0.67627	0.67629	0.67612	0.67575	0.23401	0.24724	0.25737	0.26278
2.00	0.37421	0.37456	0.37491	0.37523	0.46711	0.58511	0.69733	0.80071
3.00	0.09993	0.10079	0.10205	0.10364	0.67938	0.93542	1.18349	1.41936
4.00	-0.13867	-0.13728	-0.13502	-0.13197	0.85647	1.23978	1.61362	1.97292
5.00	-0.33148	-0.32965	-0.32653	-0.32221	0.98924	1.45772	1.91614	2.35907
6.00	-0.4655	-0.46342	-0.45979	-0.4547	1.07335	1.56549	2.04804	2.51576
7.00	-0.52403	-0.52197	-0.51834	-0.51321	1.1092	1.55568	1.99408	2.41995
8.00	-0.48562	-0.48392	-0.48089	-0.47661	1.10182	1.43739	1.76726	2.08826
9.00	-0.32274	-0.32173	-0.31995	-0.31742	1.06079	1.23709	1.41057	1.57961
10.0	0.00000	0.00000	0.00000	0.00000	1.00000	1.00000	1.00000	1.00000

4. COMPARISON OF PRESENT RESULTS WITH EXISTING SOLUTIONS

The second order linear ordinary differential equations (6 and 7) which have been obtained are coupled with velocity and temperature fields. The results of differential equations governed by the equations (6 and 7) by employing the b. c's (8 and 9) for velocity and temperature were measured using the MATHEMATICA ND solver tool package via. shooting technique with 6th order R-K methods. The solution's convergence was confirmed to meet the problem's boundary circumstances. Tables and illustrations have been used to display the impact of diverse material constants for the velocity and temperature of the fluid.

4.1 Tables

Table 3. Comparison of velocity $U(Y)$ and temperature $T(Y)$ results for b_3

Y	$U(Y)$ $V = 0, a_6 = 0.01, C_1 = 0.2, C_2 = 0.2, a_1 = 0.1, p_r = 0.77$				$T(Y)$ $V = 0, a_6 = 0.01, C_1 = 0.2, C_2 = 0.2, a_1 = 0.1, p_r = 0.77$			
	Present Results		Results of P. N. Rao *et al.* [6]		Present Results		Results of P. N. Rao *et al.* [6]	
	b3=0.10	b3=0.10	b3=0.10	b3=0.10	b3=0.10	b3=0.10	b3=0.10	b3=0.10
0.00	1.00000	1.00000	1.00000	1.00000	0.00000	0.00000	0.00000	0.00000
1.00	0.45014	0.45017	0.45011	0.45016	0.23518	0.26635	0.23520	0.26634
2.00	0.00029	0.00034	0.00020	0.00033	0.48544	0.54084	0.48545	0.54083
3.00	-0.34958	-0.3495	-0.34953	-0.34950	0.72307	0.79577	0.72300	0.79578
4.00	-0.59947	-0.59939	-0.59942	-0.59940	0.92656	1.00963	0.92655	1.00964
5.00	-0.74942	-0.74933	-0.74941	-0.74934	1.08052	1.16705	1.08049	1.16700
6.00	-0.79942	-0.79934	-0.79944	-0.79933	1.17574	1.2588	1.17575	1.25870

7.00	-0.74949	-0.74942	-0.74950	-0.74944	1.20914	1.28183	1.20913	1.28184
8.00	-0.59962	-0.59956	-0.59959	-0.59957	1.18381	1.2392	1.18379	1.23919
9.00	-0.34979	-0.34976	-0.34981	-0.34975	1.10897	1.14013	1.10900	1.14014
10.0	0.00000	0.00000	0.00000	0.00000	1.00000	1.00000	1.00000	1.00000

Table 4. Comparison of velocity $U(Y)$ and temperature $T(Y)$ results for a_6

Y	$U(Y)$				$T(Y)$			
	$V=0, b_3=0.10, C_1=0.2, C_2=0.2, a_1=0.1, p_r=0.77$				$V=0, b_3=0.10, C_1=0.2, C_2=0.2, a_1=0.1, p_r=0.77$			
	Present Results		Results of P.N. Rao *et al.* [6]		Present Results		Results of P.N. Rao *et al.* [6]	
	a6=0.01	a6=0.05	a6=0.01	a6=0.05	a6=0.01	a6=0.05	a6=0.01	a6=0.05
0.00	1.00000	1.00000	1.00000	1.00000	0.00000	0.00000	0.00000	0.00000
1.00	0.45014	0.45015	0.45015	0.45016	0.23518	0.23520	0.23519	0.23519
2.00	0.00029	0.00030	0.00030	0.00029	0.48544	0.48539	0.48545	0.48543
3.00	-0.34958	-0.34959	-0.34960	-0.34950	0.72307	0.72306	0.72308	0.72300
4.00	-0.59947	-0.59944	-0.59948	-0.59948	0.92656	0.92661	0.92659	0.92658
5.00	-0.74942	-0.74943	-0.74945	-0.74941	1.08052	1.08060	1.08060	1.08058
6.00	-0.79942	-0.79940	-0.79944	-0.79942	1.17574	1.17577	1.17579	1.17576
7.00	-0.74949	-0.74950	-0.74950	-0.74951	1.20914	1.20915	1.20918	1.20918
8.00	-0.59962	-0.59957	-0.59961	-0.59962	1.18381	1.18379	1.18380	1.18383
9.00	-0.34979	-0.34978	-0.34980	-0.34981	1.10897	1.10899	1.10898	1.10890
10.0	0.00000	0.00000	0.00000	0.00000	1.00000	1.00000	1.00000	1.00000

5. DISCUSSION ON RESULTS

The numerically obtained computations using ND solve developed in MATHEMATICA software are graphically depicted in Figs. 3–12. The problem's physical perception was seen by examining the velocity$(U(Y))$ and temperature$(T(Y))$ field results, which were acquired by assigning various values to various physical factors such suction/injection(V), coefficient of thermal interaction stress coefficient(a_6), thermal strain coefficient of conductivity (b_3), cross viscosity parameter (μ_c), Prandtl parameter(p_r), non dimensional viscosity (a_1), specific heat (c), density (ρ), constant pressure gradient (C_1) and constant temperature gradient (C_2) which characterize the flow occurrence. Graphical illustrations have been produced to show the impact of each of these coefficients on the temperature and velocity fields.

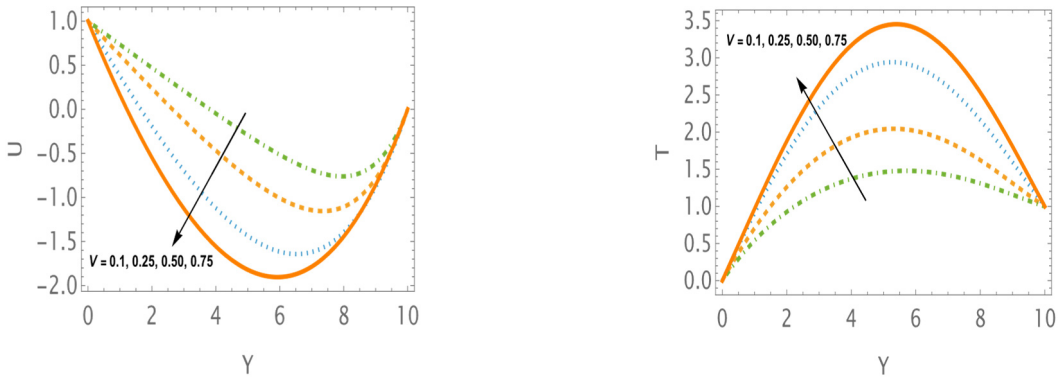

(a) (b)

Figure 3. (a) Velocity (b) Temperature contours for V with $a_6 = 0.01$ and $b_3 = 0.1$

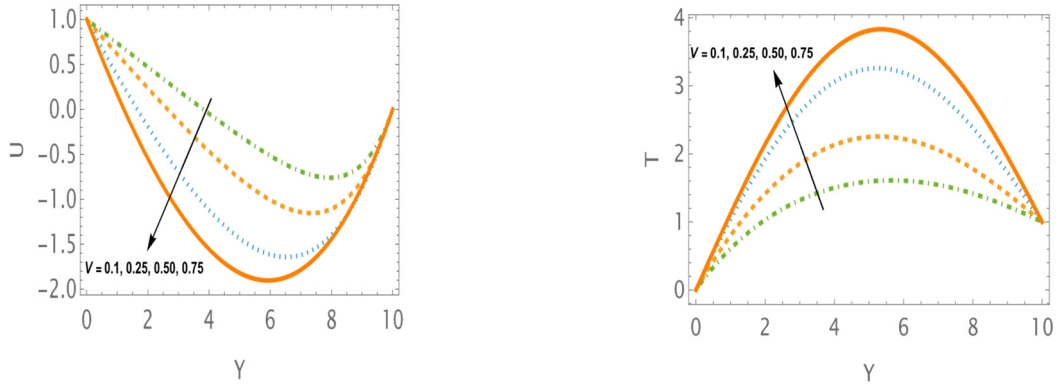

(a) (b)

Figure 4. (a) Velocity (b) Temperature contours for V with $a_6 = 0.05$ and $b_3 = 1$

In Figs. (3), (4) and (5), the variations in both $U(Y)$ and $T(Y)$ have been studied with the impact of suction/injunction parameter. The $U(Y)$ profiles are shown to decrease up to the center channel, after which they alternately decrease till the infinite distance. However, for the temperature profiles, the opposite effect has been noted. Fig. (3a and 3b) depicts the variations of $U(Y)$ besides $T(Y)$ thru the very small amount of a_6 and b_3. Fig. (4a and 4b) depicts the variations of $U(Y)$ in addition $T(Y)$ by the small rates of a_6 and b_3. Fig. (5a and 5b) depicts the variations of $U(Y)$ and $T(Y)$ with the very big values of a_6 and $T(Y)$. It is identified from the Figs. (3a 4a and 5a) that , the $U(Y)$ variations decreases as the values of V increases but as the values of b_3 increases from very small values to very large values ($i.e.0.1\ to\ 10$) there is no much variations is observed among the $U(Y)$ profiles. This effect of variation can also be observed in the Fig.(6(a)) It is depicted from the Figs. (3b, 4b and 5b) that, the $T(Y)$ variations increase as the values of V increases. For small values of b_3, the $T(Y)$ variations increase at the small rate and very large values of b_3 $T(Y)$ variations increase at the faster rate.

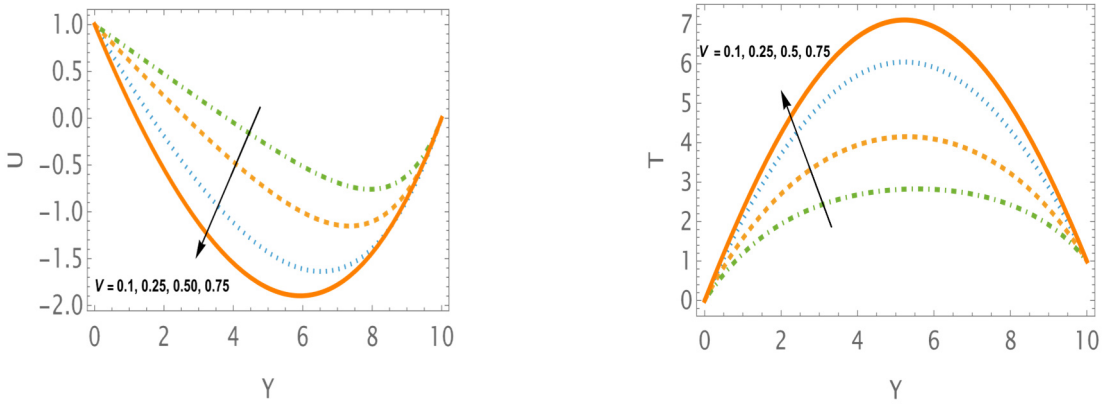

(a) (b)

Figure 5. (a) Velocity (b) Temperature contours for V with $a_6 = 0.10$ and $b_3 = 10$

The variation of $U(Y)$ also $T(Y)$ profiles in relation to b_3 effect is observed in the Figs. (6(a) and 6(b)). In Fig. 6(a), it is observed that all the $U(Y)$ profiles are coinciding. In Fig. 6(b), it is noticed that, the temperature, as the fluid move away from the plate is increasing at the faster rate up to certain distance and suddenly takes the turn and decreases to take the max. assumed temperature at the infinite distance from the plate boundary.

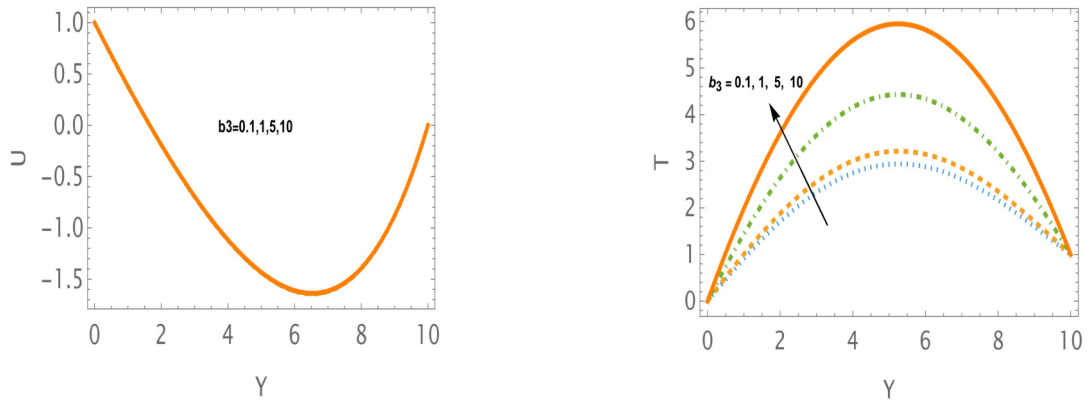

(a) (b)

Figure 6. (a) Velocity (b) Temperature contours for b_3 with $a_6 = 0.01$ and $V = 0.25$

The velocity at the center of the plates continues to decrease as the injection/suction parameter magnitude increases. This is because the non-Newtonian fluid in question has non-linear properties. Higher injection/suction parameter magnitudes will therefore lower the fluid velocity in the first half. But in the second half, these are counterbalanced by higher velocities, thus the overall impact of velocity is felt throughout the fluid's passage. Conversely, with lower magnitudes, the velocity increases more in the first half and less in the second. Additionally, it should be noted that the curves join at the bottom and top in all cases. This is due to the condition that prevails on the surfaces as the fluid flows.

The effect of a_6 on the $U(Y)$ and $T(Y)$ profiles is noted in the Figs. (7(a) and 7(b)). In Fig. 7(a), it is noted that all the $U(Y)$ profiles are overlaps each other. After decreasing till the centre, the velocity steadily increases until it influences the endless flow area. The temperature of the fluid is drastically increasing up to middle distance and suddenly drops then decreases to take the max. temperature.

The result of constant pressure gradient on $U(Y)$ and $T(Y)$ with different values for small values of b_3 and V have been shown in Figs. 8(a) and 8(b). Completely opposite effects have been observed on $U(Y)$ and $T(Y)$ profiles. The velocity reduced and the temperature raised as the constant pressure gradient values increases with the small values. The

velocity variations are completely drifting down the plate where as the temperature variations are drifting up from surface of the plate.

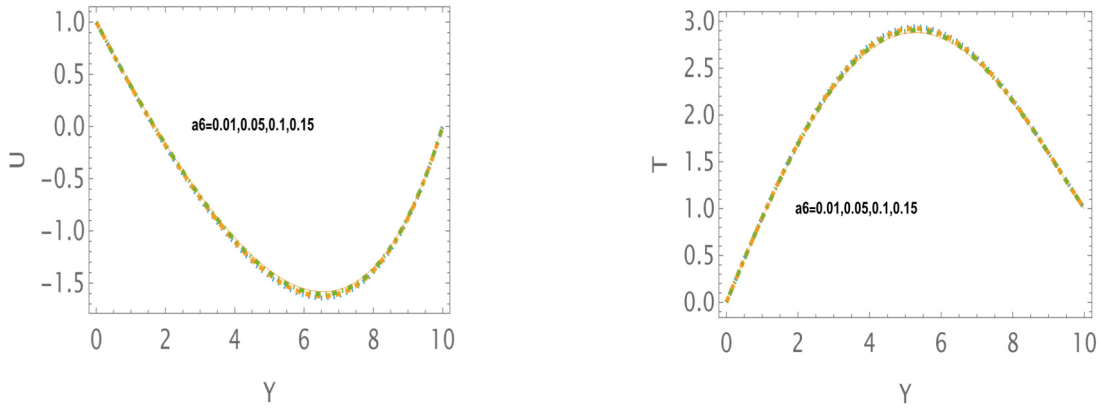

(a) (b)

Figure 7. (a) Velocity (b) Temperature contours for a_6 with $b_3 = 0.1$ and $V = 0.25$

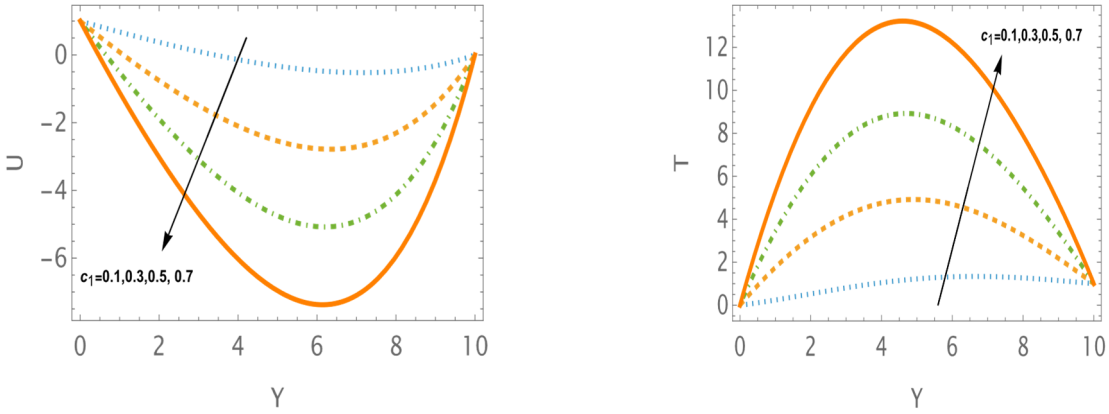

(a) (b)

Figure 8. (a) Velocity (b) Temperature contours for C_1 with $b_3 = 0.1$ and $V = 0.25$

The impact of constant temperature gradient on $U(Y)$ besides $T(Y)$ by different values for small values of b_3 and V have been shown in Figs. 9(a) and 9(b). All the velocity variations overlap for the values of constant temperature gradient increases. Completely opposite effects have been observed on $U(Y)$ and $T(Y)$ profiles. As the constant temperature gradient values rise with the very small values, the temperature rises and the velocity falls. Whereas the temperature variations are migrating upward from the plate's surface, the velocity variations are entirely drifting downward.

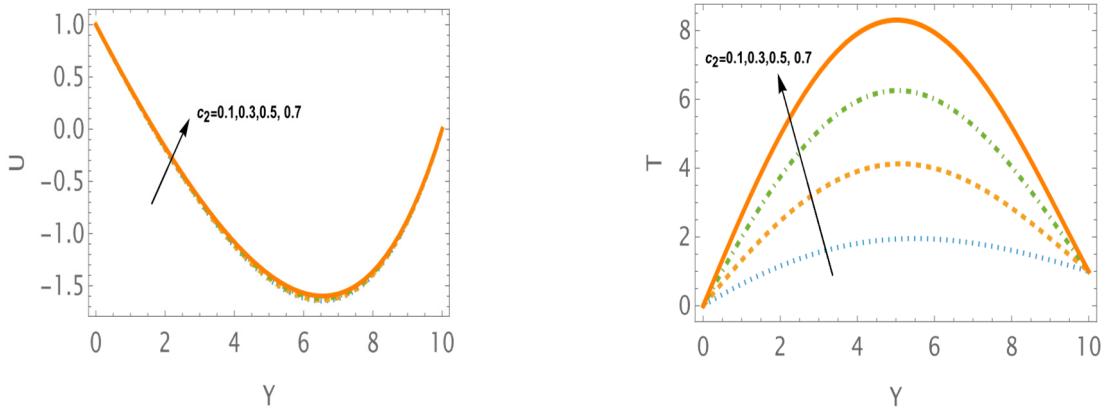

(a) (b)

Figure 9. (a) Velocity (b) Temperature contours for C_2 with $b_3 = 0.1$ and $V = 0.25$

The dimensionless viscosity coefficient(a_1) influence on both $U(Y)$ and $T(Y)$ is shown in Figs. 10(a), 10(b) and 10(c). The $T(Y)$ profiles rise strongly until the middle flow zone, after which they fall to reach the maximum temperature far from the plate surface, while the $U(Y)$ profiles coincide. When b_3 is large, the rate of temperature increase is higher; when b_3 is small, the rate of temperature increase is lower.

The influence of small Prandtl (p_r) number values on $U(Y)$ and $T(Y)$ is shown in Figs. 11(a) to 11(d). The variation of (p_r) values on velocity also not shown much effect and all $U(Y)$ profiles coincide with this effect. The $T(Y)$ variations with increase of small p_r values increase and is observed in figs. 11(b) to 11(d). It is also noted that, the temperature variations increase with the increase of very small values of b_3 to the very large values of b_3 .

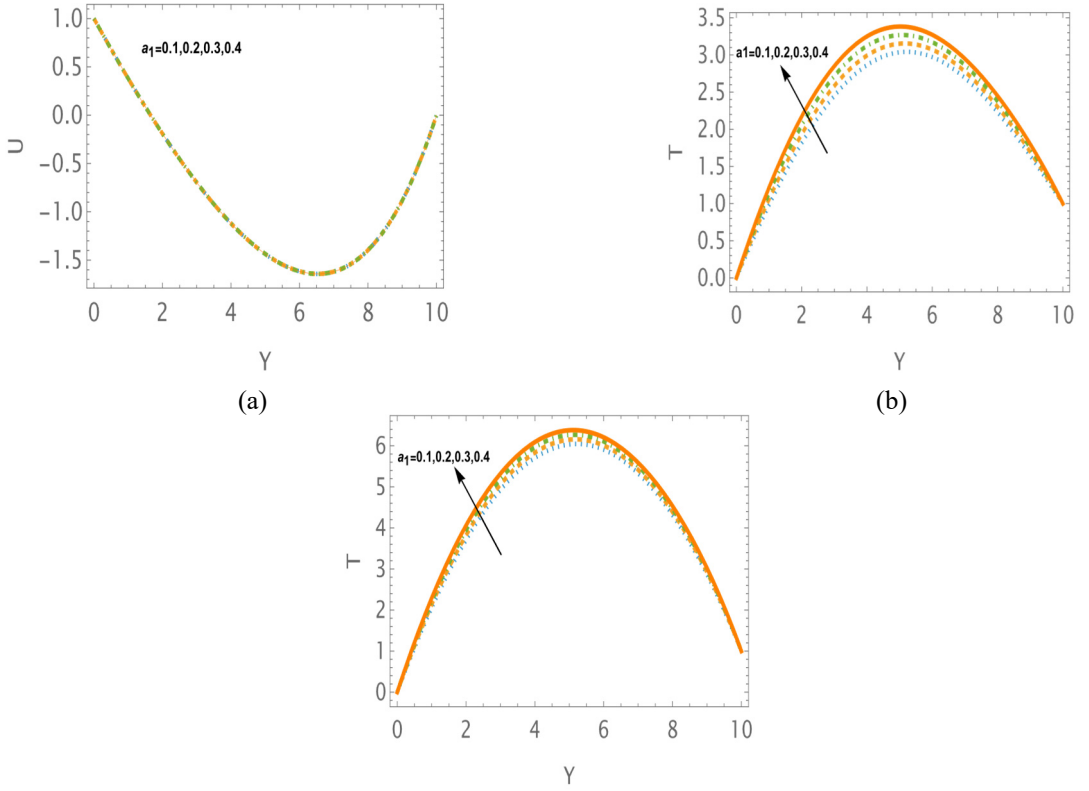

Figure 10. (a) Velocity for $b_3 = 0.1$ and (b), (c) Temperature for $b_3 = 0.1$ and $b_3 = 10$

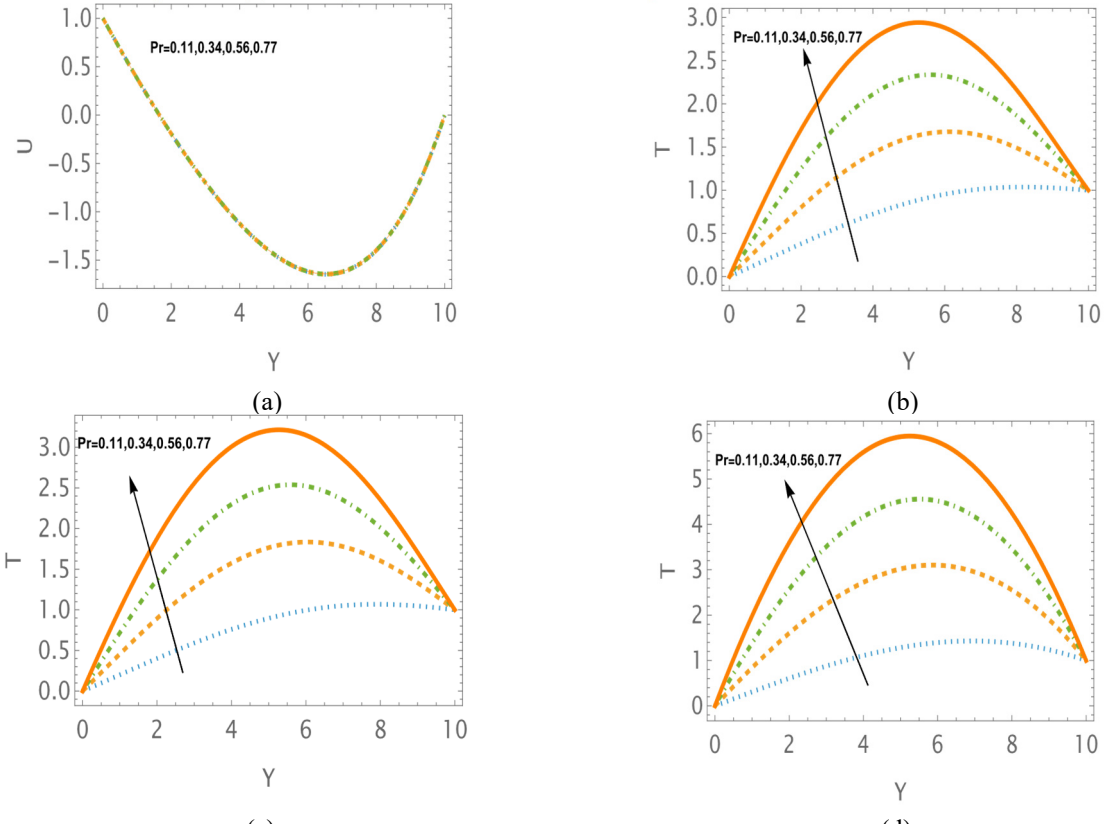

Figure 11. (a) Velocity for $b_3 = 0.1$ and (b), (c) , (d) Temperature for small p_r with $b_3 = 0.1$, $b_3 = 1$ and $b_3 = 10$

The maximum temperature parameter has consistently produced a high thermal conductivity, albeit to varied degrees. Accordingly, it is possible to say that the thermal conductivity of non-Newtonian materials is directly proportional to the Y-location. However, this is only part of the reality. According to the fluid domain's overall spatial view, temperature variations were shifted from the upper triangle to the lower triangle as the thermal conductivity factor grew from 0.1 to 10.0. This is because the fluid under consideration is non-homogeneous and anisotropic. The thermal conductivity influence will differ depending on the location due to the anisotropic nature. The associated figures clearly show this.

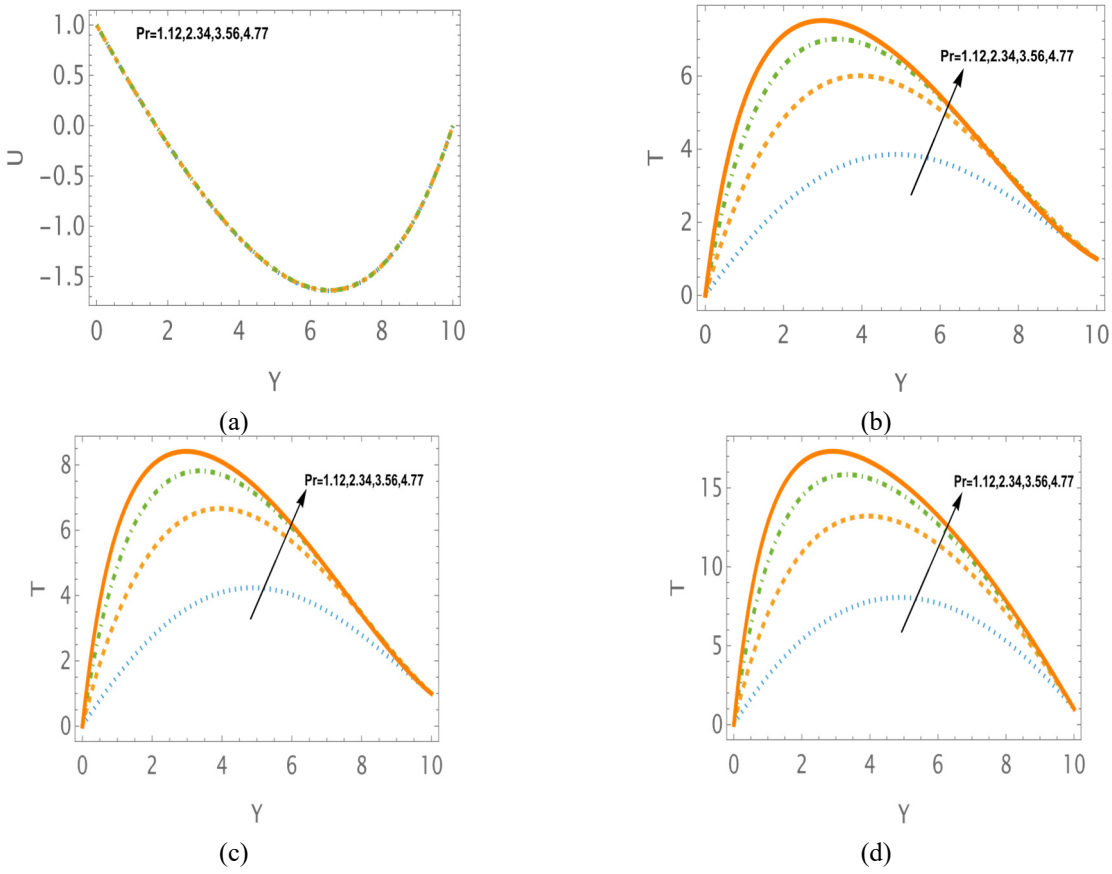

Figure 12. (a) Velocity for $b_3 = 0.1$ and (b), (c), (d) Temperature for big p_r with $b_3 = 0.1$, $b_3 = 1$ and $b_3 = 10$

The influence of big Prandtl (p_r) number values on $U(Y)$ and $T(Y)$ is shown in Figs. 12(a) to 12(d). Additionally, there is little effect of the changing of p_r values on velocity, and all $U(Y)$ profiles coincide with this effect. The $T(Y)$ variations with increase of small p_r values increase and is observed in figs. 12(b) to 12(d). It is also noted that, the temperature variations increase with the increase of very small values of b_3 to the very large values of b_3 . The temperature increases more quickly when the p_r values rise from modest to big levels.

In the design of aircraft wings, the behavior of the thermo-viscous boundary layer across a flat plate is greatly influenced by temperature dependent material qualities, such as viscosity, thermal conductivity, and specific heat. Because of the friction with the wing surface, the air usually becomes less viscous as it heats up, changing the velocity profile and perhaps postponing flow separation. The thermal boundary layer forms concurrently, and its thickness is determined by the air's specific heat and thermal conductivity. While a fluid with a greater specific heat can absorb more heat before its temperature increases noticeably, a fluid with a higher thermal conductivity can dissipate heat more quickly.

6. CONCLUSIONS

This study presents a novel numerical approach for analysis on thermo-viscous steady fluid motion through the moving rectangular plate for an application of aircraft wing design in aerospace engineering. The governing equations numerical solution has been found, and the MATHEMATICA ND solver tool with 6th order R-K techniques has used to solve the resulting governing equations. For a range of physical values of different parameters, as well as for some fixed values of other coefficients, the solutions are implemented.

- The suction parameter/ injection (V) factor decreases the fluid's velocity and increases the temperature. The opposite effects have been noted on both the velocity and the temperature.
- When the coefficient of heat conductivity (b_3) grows to large levels, the fluid velocity increases more quickly.

- Thermal conductivity (b_3) and thermal stress mechanical interaction (a_6) decreases the fluid's velocity and increases the temperature.
- The dimensionless viscosity coefficient (a_1), constant pressure and temperature gradients increase the temperature. There is no variation in velocity with these parameters' effects.
- The small and big values of the Prandtl number (p_r) increases both the velocity and the temperature.
- The derived numerical solutions show an excellent agreement with the available analytical solutions in the literature.
- The parameters of heat transport and the boundary layer over aircraft surfaces are greatly influenced by the temperature-dependent material properties of thermo-viscous fluids.

ORCID

N. Pothanna, https://orcid.org/0000-0003-3983-3125; **P. Raja Shekar,** https://orcid.org/0000-0003-4028-4688; **Jyotsna Cherukuri,** https://orcid.org/0000-0002-9861-7978; **L. Srinivasa Rao,** https://orcid.org/0000-0001-9249-1713; **Adigoppula Raju**, https://orcid.org/0000-0002-8927-3376, **Devunuri Suresh**, https://orcid.org/0000-0002-0533-8604

REFERENCES

[1] S.L. Koh, and A.C. Eringen, "On the foundations of non-linear thermo-viscoelasticity," International Journal of Engineering Science, **1**(2), 199-229 (1963). https://doi.org/10.1016/0020-7225(63)90034-X
[2] K. Yamamoto, and Z.-I. Yoshida, "Flow through a porous wall with convective acceleration," Journal of the Physical Society of Japan, **37**(3), 774-779 (1974). https://doi.org/10.1143/JPSJ.37.774
[3] S.B. Gordon, and D.D. Joseph, "Boundary conditions at a naturally permeable wall, Journal of fluid mechanics," **30**(1), 197-207 (1967). https://doi.org/10.1017/S0022112067001375
[4] D.C. Bernard, and J.V. Mizel, "Existence of caloric equations of state in thermodynamics," The Journal of Chemical Physics, **40**(4), 1116-1125 (1964). https://doi.org/10.1063/1.1725257
[5] P.D. Kelly, "Some viscometric flows of incompressible thermo viscous fluids," International Journal of Engineering Science, **2**(5), 519-533 (1965). https://doi.org/10.1016/0020-7225(65)90007-8
[6] P.N. Rao, and N.Ch. Pattabhiramacharyulu, "Steady flow of a second-order thermo-viscous fluid over an infinite plate," in: *Proceedings of the Indian Academy of Sciences-Mathematical Sciences*. **88**, 157-161 (1979). (Springer India). https://doi.org/10.1007/BF02871612
[7] N. Pothanna, and P. Aparna, "Unsteady thermo viscous flow in a porous slab over an oscillating flat plate," J. Porous Media, **22**, 531–543 (2019). https://doi.org/10.1615/JPorMedia.2019028871
[8] G.J. Reddy, P. Mangathai, and N. Pothanna, "Analysis of heat generation impact on nanofluid flow over a stretching sheet," Partial Differential Equations in Applied Mathematics, **11**, 100852 (2024). https://doi.org/10.1016/j.padiff.2024.100852
[9] N. Pothanna, P. Aparna, M.P. Reddy, R.A. Reddy, and M.C.J. Anand, "Thermo-viscous fluid flow in porous slab bounded between two impermeable parallel plates in relative motion: Four stage algorithm approach," Applications of Mathematics, **69**, 807–827 (2024). https://doi.org/10.21136/AM.2024.0144-23
[10] M.A. Kumar, N. Pothanna, and G.J. Reddy, "Analyzing the heat and mass transfer behavior in a 2-D forchheimer porous medium on MHD Casson fluid flow over an inclined non-linear surface with viscous dissipation, chemical reaction, and Soret–Dufour parameters," Multiscale and Multidiscip. Model. Exp. and Des. **8**, 176 (2025). https://doi.org/10.1007/s41939-025-00767-6
[11] N. Pothanna, "Investigation on unsteady fluid flow around an oscillating sphere-A numerical and analytical approach," Hybrid Advances, **6**, 100257 (2024). https://doi.org/10.1016/j.hybadv.2024.100257
[12] P.R. Shekar, G.J. Reddy, and N. Pothanna, "Influence of Thermal Radiation on MHD Casson Nanofluid Flow over a Non-Linear Stretching Sheet with the Presence of Chemical Reaction," East European Journal of Physics, (1), 101-111 (2025). https://doi.org/10.26565/2312-4334-2025-1-09
[13] N. Pothanna, J. Srinivas, C. Thirmal, G.R. Chandra, and L.S. Raj, "Unsteady thermo viscous fluid motion between two infinitely extended impermeable horizontal plates-an artificial neural networks approach," Thermal Science and Engineering Progress, **62**, 103617 (2025). https://doi.org/10.1016/j.tsep.2025.103617
[14] P. Nalimela, C. Thirmal, V.G. Kumar, and G.J. Reddy, "Artificial neural networks analysis of an unsteady fluid flow through a horizontal oscillating flat plate in a porous slab," Physics of Fluids, **37**, (2025). https://doi.org/10.1063/5.0253605
[15] A. Naeem, Z. Abbas, and M.Y. Rafiq, "Radially inflows and outflows of hydromagnetic viscous fluid between two narrowly flat disks," Results in Engineering, **25**, 103924 (2025). https://doi.org/10.1016/j.rineng.2025.103924
[16] T. Naseem, F. Mebarek-Oudina, H. Vaidya, N. Bibi, K. Ramesh, and S.U. Khan, "Numerical Analysis of Entropy Generation in Joule Heated Radiative Viscous Fluid Flow over a Permeable Radially Stretching Disk," CMES - Computer Modeling in Engineering and Sciences, **143**(1), 351-371 (2025). https://doi.org/10.32604/cmes.2025.063196
[17] Z.I. Butt, I. Ahmad, M. Shoaib, H. Ilyas, and M.A.Z. Raja, "Electro-magnetohydrodynamic impact on Darrcy-Forchheimer viscous fluid flow over a stretchable surface: Integrated intelligent Neuro-evolutionary computing approach," International Communications in Heat and Mass Transfer, **137**, 106262 (2022). https://doi.org/10.1016/j.icheatmasstransfer.2022.106262
[18] H. Milosevic, N.A. Geydarov, Y.N. Zakharov, and S. Stevovic, "Model of incompressible viscous fluid flow driven by pressure difference in a given channel," International Journal of Heat and Mass Transfer, **62**, 242-246 (2013). https://doi.org/10.1016/j.ijheatmasstransfer.2013.02.059
[19] N. Fatima, K.S. Nisar, S. Shaheen, M.B. Arain, N. Ijaz, T. Muhammad, "A case study for heat and mass transfer of viscous fluid flow in double layer due to ciliated channel," Case Studies in Thermal Engineering, **45**, 102943 (2023). https://doi.org/10.1016/j.csite.2023.102943
[20] A.M. Saleem, N.M. Basher, and A.A. Yousif, "Effect of suction or blowing on velocity and temperature distribution of flow over a flat plate," Materials Today: Proceedings, **42**(5), 2859-2865 (2021). https://doi.org/10.1016/j.matpr.2020.12.735

[21] J. Jayaprakash, and V. Govindan, "Impacts of diffusion and chemical reaction on heat transfer in Casson nanofluids flow over a flat plate with accretion," Case Studies in Thermal Engineering, **72**, 106309 (2025). https://doi.org/10.1016/j.csite.2025.106309
[22] S. Peng, T. Peng, Y. Feng, and X. Zheng, "Compressible magnetohydrodynamic flat plate boundary layer flow with slightly rarefied effects," European Journal of Mechanics-B/Fluids, **113**, 204281 (2025). https://doi.org/10.1016/j.euromechflu.2025.204281
[23] W. Zeng, Y. Fang, and H. Ma, "Use of Multi-Test Strategy to Obtain Heat Transfer Coefficient and Adiabatic Wall Temperature Simultaneously in Shock Tunnel for Transonic Flow over a Flat Plate," Aerospace Science and Technology, **160**, 110057 (2025). https://doi.org/10.1016/j.ast.2025.110057
[24] S. Nadeem, W. Fuzhang, F.M. Alharbi, F. Sajid, N. Abbas, A.S. El-Shafay, and F.S. Al-Mubaddel, "Numerical computations for Buongiorno nano fluid model on the boundary layer flow of viscoelastic fluid towards a nonlinear stretching sheet," Alexandria Engineering Journal, **61**(2), 1769-1778 (2022). https://doi.org/10.1016/j.aej.2021.11.013
[25] A.A. Azar, "Thermal radiation and magnetic field effects on dusty hyperbolic tangent fluid flow over a stretching sheet with high Prandtl number," International Communications in Heat and Mass Transfer, **165**, Part A, 109040 (2025). https://doi.org/10.1016/j.icheatmasstransfer.2025.109040
[26] I. Ullah, S. Shafie, and I. Khan, "Effects of slip condition and Newtonian heating on MHD flow of Casson fluid over a nonlinearly stretching sheet saturated in a porous medium," Journal of King Saud University – Science, **29**(2), 250-259 (2017). https://doi.org/10.1016/j.jksus.2016.05.003
[27] H.R. Kataria, and H.R. Patel, "Heat and mass transfer in magnetohydrodynamic (MHD) Casson fluid flow past over an oscillating vertical plate embedded in porous medium with ramped wall temperature," Propulsion and Power Research, **7**(3), 257-267 (2018). https://doi.org/10.1016/j.jppr.2018.07.003
[28] S.M. Ibrahim, G. Lorenzini, P.V. Kumar, and C.S.K. Raju, "Influence of chemical reaction and heat source on dissipative MHD mixed convection flow of a Casson nanofluid over a nonlinear permeable stretching sheet," International Journal of Heat and Mass Transfer, **111**, 346-355 (2017). https://doi.org/10.1016/j.ijheatmasstransfer.2017.03.097
[29] C. Fetecau, and C. Fetecau, "A new exact solution for the flow of a Maxwell fluid past an infinite plate," International Journal of Non-Linear Mechanics, **38**(3), 423-427 (2003). https://doi.org/10.1016/S0020-7462(01)00062-2
[30] S. Dholey, "Flow due to an infinite flat plate suddenly set into motion in a viscoelastic fluid: first Stokes problem," Sadhana, **44**, 118 (2019). https://doi.org/10.1007/s12046-019-1098-9

ДОСЛІДЖЕННЯ ТЕРМО-В'ЯЗКОГО СТАЦІОНАРНОГО РУХУ РІДИНИ ЧЕРЕЗ РУХОМУ ПРЯМОКУТНУ ПЛОСКУ ПЛАСТИНУ – ЧИСЛОВИЙ ПІДХІД

Н. Потханна[1], П. Раджа Шекар[1], Джйотсна Черукурі[2], Л. Срінівас Рао[3], Адігоппула Раджу[4], Девунурі Суреш[5]

[1]Кафедра математики, Інженерно-технологічний інститут ім. ВНР Віньяна Джйоті, Хайдерабад, Телангана, Індія-500090
[2]Кафедра хімії, Інженерно-технологічний інститут ім. ВНР Віньяна Джйоті, Хайдерабад, Телангана, Індія-500090
[3]Центр нанонауки та технологій, кафедра фізики, Інженерно-технологічний інститут ім. ВНР Віньяна Джйоті, Бачупаллі, ГІД., ТГ, Індія-500 090
[4]Кафедра прикладних наук, Технологічний інститут Симбіозу, Symbiosis International (вважається Університет), Пуне-412115, Індія
[5]Кафедра автомобільної інженерії, Інститут інженерії та технологій VNR Віньяна Джйоті, Хайдерабад, Телангана, Індія-500090

Це дослідження представляє новий числовий підхід до аналізу руху термов'язкої стаціонарної рідини через рухому прямокутну плоску пластину. Числові результати були отримані з використанням методу Рунге-Кутти 6-го порядку, розробленого в програмному забезпеченні Mathematica. Числове диференціювання розв'язує адаптивні рівняння потоку, що включають температуру та швидкість. Поведінка потоку та вплив матеріальних обмежень на область потоку для керованих рівнянь були проаналізовані та розглянуті за допомогою згенерованих графіків. Нелінійні зв'язані диференціальні рівняння з частинними похідними (ДРП) щодо температури та швидкості, з урахуванням відповідних граничних умов, керують рухом рідини. Числові розрахунки результатів Рунге-Кутти (Р-К) 6-го порядку представлені у вигляді таблиць, а також для численних значень теплофізичних коефіцієнтів. Варіації цих полів потоку були досліджені для широкого спектру фізичних характеристик, які впливають на природу термов'язкої рідини. Вплив параметра всмоктування/впорскування, безрозмірного коефіцієнта в'язкості, постійних градієнтів тиску та температури, теплофізичних факторів та впливу параметра Прандтля на область потоку було досліджено за допомогою графічних ілюстрацій з широким діапазоном значень. Також були проведені чіткі числові розрахунки, результати яких пов'язані з сучасними результатами в літературі. Для покращення швидкості теплопередачі в таких системах, як теплообмінники та аерокосмічні компоненти, інженери можуть оптимізувати текстури поверхні та умови потоку, враховуючи вплив коефіцієнтів на міркування потоку.

Ключові слова: *термов'язка рідина; розв'язання ND; метод R-K 6-го порядку; проникність; теплопровідність*